Investigating the Potential of Long Time Series Remote Sensing NDVI datasets for Forest Gross Primary Productivity Estimation over Continental U.S.

Xiaolei Yu
Department of Geography and Planning
University of Saskatchewan
Kirk Hall 117 Science Place
Saskatoon SK, S7N 5C8
Canada

School of Remote Sensing and Information Engineering
Wuhan University, No. 129, Luoyu Road
Wuhan Hubei, 430079
China

Xulin Guo
Department of Geography and Planning
University of Saskatchewan
Kirk Hall 117 Science Place
Saskatoon SK, S7N 5C8
Canada

Zhaocong Wu
School of Remote Sensing and Information Engineering
Wuhan University, No. 129, Luoyu Road
Wuhan Hubei, 430079
China

Abstract

*Several global remote sensing normalized difference vegetation index (NDVI) datasets have been established for vegetation monitoring and climate change study, including the MODIS NDVI product, the GIMMS and so on. Many researches focused on estimating forest gross primary productivity (GPP) by MODIS data, which is only available from 2000. However, the GIMMS dataset has a long record period from 1981 to 2006, and will be continued to most recent year (GIMMS3g). That is very suitable for long time period GPP monitoring. Nonetheless, there is a lack of comparison between those two different NDVI datasets for forest GPP estimation. As an attempt to deal with that problem, MOD13A1 from MODIS and GIMMS from AVHRR were used in this study to test the potential of NDVI for forest GPP estimation over continental U.S. from the greenness and radiation (GR) model. Meanwhile, three different predictors: NDVI, NDVI*NDVI and NDVI*NDVI*PAR were chosen to accompany with linear, quadratic and exponent functions for GPP estimation at 15 Ameriflux sites. Results showed that both MODIS and AVHRR NDVI datasets have the ability to predict GPP. However, the MODIS data outperforms AVHRR data. Meanwhile, the predictor of NDVI*NDVI*PAR has better explanatory power than others. As for three statistical models, no one is obvious better than others.*

Keywords: GPP; NDVI; MODIS; AVHRR; GIMMS; Ameriflux

1. Introduction

Gross Primary Productivity (GPP), defined as the amount of carbon fixed by vegetation through photosynthesis, is a key component of ecosystem carbon fluxes and the carbon balance between the biosphere and the atmosphere (MÄKELÄ et al., 2008).

Quantification of the magnitude of (C) uptake, and how it varies inter-annually, is an important question with future potential sequestration influenced by both increased atmospheric CO2 and changing climate (Nemani et al., 2003). Therefore, the accurate estimation of GPP is essential for the quantification of net terrestrial carbon, which is often a small difference of two large carbon fluxes:

GPP and ecosystem respiration (Re) (X. Xiao et al., 2004). Estimation of GPP for terrestrial ecosystems at region, continent, or the globe level can improve our understanding of the feed-backs between the terrestrial biosphere and the atmosphere in the context of global change and facilitate climate policy-making (J. Xiao et al., 2008). However, this can only be fulfilled by using ecosystem models (Prince & Goward, 1995) or remotely sensed approaches (Running, Thornton, Nemani, & Glassy, 2000). A number of remote sensing based productivity estimation models have been proposed. Early approaches include the Carnegie Ames Stanford Approach Biosphere model (CASA) (Potter et al., 2003), the Global Production Efficiency Model (GLO-PEM) (Ruimy, Kergoat, & Bondeau, 1999) and the Bio-Geochemical Cycles model (BGC) (Running & Gower, 1991), which require relatively more parameters as the model inputs. The simplified BGC model has been used for Moderate Resolution Imaging Spectroradiometer (MODIS) product termed MOD17 generation (M. Zhao, Running, & Nemani, 2006), and it still requires considerable inputs from meteorological measurements and lookup tables based on vegetation types. These can introduce errors into GPP estimation, either in the original estimate of LUE for a particular vegetation type or in the assignment of vegetation type to one pixel, since these input data are not often available at the same spatial or temporal scale as the remote sensing imagery .

Recent studies focus on the light use efficiency (LUE) model, which is supposed to have the highest potential for adequately addressing the spatial and temporal GPP dynamics. It proposes a direct proportional relation between biological production and the amount of photosynthetically active radiation (PAR) absorbed by the vegetation canopy (APAR) (Sims et al., 2008).The fundamental methodology of GPP estimation is based on former research (Monteith, 1972; Monteith & Moss, 1977) as:

$$GPP = LUE * f_{APAR} * PAR \qquad (1)$$

where fAPAR represents the fraction of absorbed PAR. The multiplication of fAPAR and PAR equals to APAR. The Vegetation Photosynthesis Model (VPM) (Monteith & Moss, 1977; X. Xiao et al., 2004) and the Physiological Principles for Predicting Growth (3-PG) model (Coops, Waring, & Law, 2005) and the EC-LUE model (W. Yuan et al., 2010; W. P. Yuan et al., 2007) also use the basic idea of equation 1. Though models driven by a large number of input parameters can give good estimates of GPP, the demand of these variables at required temporal and spatial resolutions is often a bottleneck for the global applications of these models (C. Wu, Niu, & Gao, 2010).

Simple algorithms are needed for GPP estimation at decent spatial scale for long time period in order to monitor the ecosystem carbon dynamic. Based on LUE model, that demands proper indicators for LUE and fAPAR. Vegetation indices (VIs) derived from one or more bands of reflectance offer important and convenient measurements for the estimation of ecosystem biophysical (e.g. Leaf area Index (LAI)) and biochemical parameters (e.g. chlorophyll content) , since these parameters are the proxy for LUE and fAPAR. These results provided the potential for estimating GPP from the combination of such VIs and climate variables . Therefore, VIs are frequently used in GPP estimation models. Commonly used VIs include Normalized Difference Vegetation Index (NDVI) (Myneni, Hall, Sellers, & Marshak, 1995), Enhanced Vegetation Index (EVI) (Salomonson, Barnes, Xiong, Kempler, & Masuoka, 2002), (Anatoly A Gitelson, Viña, Masek, Verma, & Suyker, 2008), wide dynamic range Vegetation Index (WDRVI) (Anatoly A Gitelson et al., 2008) and so on. Among these VIs, NDVI has the widest usage and relatively long history (Holben, 1986), nevertheless is has some limitation for different situations (Jiang, Huete, Didan, & Miura, 2008).

The greenness radiation (GR) model proposed by Wu *et al.* suggests that GPP can be predicted by the combination of EVI and PAR (C. Wu, Chen, & Huang, 2011; C. Wu, Niu, et al., 2010; C. Wu et al., 2009). This model has been applied for various ecosystems types using MODIS EVI data (C. Wu, Gonsamo, Zhang, & Chen, 2014). Most researches focus on the MODIS dataset for GPP prediction, only covering the time period from 1999. While the Global Inventory Modeling and Mapping Studies (GIMMS) dataset from Advanced Very High Resolution Radiometer (AVHRR) has a long-term record for NDVI from 1981 (Julien & Sobrino, 2009), which has been improved and extended as GIMMS3g to recent years (Fensholt & Proud, 2012).

That can provide us a long term knowledge for GPP estimation. Therefore, in this paper, we investigated the potential of NDVI from MODIS and GIMMS for forest GPP estimation over continental U.S. based on the theory of GR model.

2. Data and Methods

The overall approach of this paper was to test if the theory of GR model can be transplanted for the NDVI datasets from MODIS and GIMMS. In the following parts, we describe: (1) the selection of study sites and processing of Ameriflux data, (2) the selection and processing of NDVI data from MODIS and AVHRR, (3) our analytical approach.

Figure 1: Map of Selected Ameriflux Forest Sites in this Study

2.1. Study Sites and Ameriflux Data

Fifteen forest sites were selected in this study, including 6 deciduous broadleaf forest sites, 6 evergreen needleleaf forest sites and 3 mixed forest sites from Ameriflux (http://ameriflux.ornl.gov/). These sites (Figure 1) represent a wide diversity of natural forest vegetation across the U.S., with considerable variation in regions, climate and species composition. Scaling from the ground measurements at the site to the remote sensing satellite image pixel is not trivial because the heterogeneity of the flux tower footprint can lead to a time-variant measurement bias (Hashimoto et al., 2012). We selected sites with no fierce land cover change according to the additional information provides by their principle investigators to avoid scaling issues and ensure selected sites with land cover extended homogeneously over a nearly 300 m radius circle around the flux tower. The specific information for those 15 sites is listed as Table 1.

Eddy flux measurements of CO_2, H_2O and energy were made as core measurements at those sites. However the data collection and duration period are not uniform (Table 1 and Figure 2). Only Level 4 Ameriflux data were used in the study, including meteorological, eddy covariance flux data and estimated GPP. The GPP was derived from estimated Net Ecosystem Exchange (NEE). The partitioning of the measured NEE fluxes into GPP and Total Ecosystem Respiration (TER) was based on a temperature-dependent exponential model of TER, using nighttime NEE data . GPP was finally obtained as the sum of NEE and TER according to Reichstein *et al.* (Reichstein et al., 2005). Both NEE and GPP were filled using the Marginal Distribution Sampling (MDS) method and the Artificial Neural Network (ANN) method (Papale & Valentini, 2003; Reichstein et al., 2005). And the time-series were finally gap-filled at the daily, weekly, and monthly time scale. Due to the reliability issue of MDS method and ANN methods, we used the results from MDS method filled data. Since the former methods handled original storage of data, which is more reliable, while the latter method was used for long time period data gap(Sims et al., 2008).

Daily data of air temperature, soil temperature, precipitation, net incident shortwave radiation (SWR), vapor pressure deficit (VPD) are provided by researchers at these 15 sites. The SWR are converted to PAR by Equation 2 (Running, Nemani, Glassy, & Thornton, 1999):

$$PAR = 0.45 * SWR \quad (2)$$

2.2. MODIS NDVI dataset (MOD13A1)

MODIS NDVI dataset is synthesized on a 16 day basis from the end of 1999, since when the satellite of TERRA was launched (Gallo, Ji, Reed, Dwyer, & Eidenshink, 2004). It carried the MODIS sensor, and followed by another identical MODIS sensor, carried by the satellite of AQUA, launched in 2002. This NDVI dataset is derived from bands 1 and 2 of MODIS, centered at 645nm, and 858nm (Table 2), as the original definition of NDVI in Equation 3:

$$NDVI = \frac{r_{nir} - r_{red}}{r_{nir} + r_{red}} \quad (3)$$

Table 1: Information for Selected Ameriflux Forest Sites

Forest Type	Site Name	Abbreviation	Latitude(°N)	Longitude(°E)	Data Period	Main Species	Citation
Deciduous Broadleaf Forest (DF)	Bartlett Experimental Forest	US-Bar	44.065	-71.288	2004- 2012	red maple, American beech, paper birch, eastern hemlock	Richardson, A.D. *et al.* (Richardson et al., 2007)
	Harvard Forest	US-Ha1	42.538	-72.171	1992- 2011	red oak, red maple, black birch , white pine, and hemlock	Wofsy, S. *et al.* (Wofsy et al., 1993)
	Ohio Oak Openings	US-Oho	41.555	-83.844	2005	northern red oak, white oak , black oak, and red maple	Abella, S.R. *et al.* (Abella et al., 2001)
	Willow Creek	US-WCr	45.806	-90.080	1998 - 2010	sugar maple, tulip poplar, sassafras, white oak, black oak	Bolstad, P. *et al.* (Bolstad, Davis, Martin, Cook, & Wang, 2004)
	Missouri Ozark	US-MOz	38.744	-92.200	2004 - 2009	northern red oak, eastern redcedar, shagbark hickory	Yang, B. *et al.* (Yang et al., 2007)
	UMBS	US-UMB	45.560	-84.714	1999 -2012	bigtooth aspen, quaking aspen, western white pine, northern red oak	Curtis, P.S. *et al.* (Curtis et al., 2002)
Evergreen Needleleaf Forest (EF)	Howland Forest Main	US-Ho1	45.204	-68.740	1996 - 2004	red spruce, eastern hemlock	Hollinger, D. *et al.* (Hollinger et al., 1999)
	North Carolina Loblolly Pine	US-NC2	35.803	-76.668	2005 - 2010	loblolly Pine	DeForest, J. *et al.* (DeForest et al., 2006)

Table 1: Information for Selected Ameriflux Forest Sites, Continued

Forest Type	Site Name	Abbreviation	Latitude(°N)	Longitude(°E)	Data Period	Main Species	Citation
Evergreen Needleleaf Forest (EF)	Austin Cary	US-SP1	29.738	-82.219	1999-2001, 2003, 2005-2008	longleaf pine, slash pine	Gholz, H. *et al.* (Gholz et al., 1991)
	Niwot Ridge	US-NR1	40.0329	-105.546	1998 -2009	subalpine fir, engelmann spruce, lodgepole pine	Turnipseed, A. *et al.* (Turnipseed, Blanken, Anderson, & Monson, 2002)
	Wisconsin Intermediate Red Pine	US-Wi2	46.687	-91.153	2003	red pine	Brosofske, K. *et al.* (Brosofske, Chen, & Crow, 2001)
	Blodgett Forest	US-Blo	38.895	-120.633	1998 -2006	ponderosa pine	Goldstein, A.H. *et al.* (Goldstein & Schade, 2000)
Mixes Forest (MF)	Fort Dix	US-Dix	39.971	-74.435	2005 -2008	pitch pine , black oak , dwarf chinkapin oak , white oak	Clark, K.L. *et al.* (Clark et al., 2009)
	Sylvania Wilderness	US-Syv	46.242	-89.348	2002 -2008	sugar maple, eastern hemlock, yellow birch, American basswood and hophornbeam	Desai, A.R. *et al.* (Desai, Bolstad, Cook, Davis, & Carey, 2005)
	Little Prospect Hill /	US-LPH	42.542	-72.185	2003-2004	red oak, red pine, white pine , eastern hemlock,red maple	Hadley, J.L. *et al.* (Hadley et al., 2008)

Where r_{nir} represents the reflectance of near infrared band and r_{red} represents the visible red band. The Terra MODIS Vegetation Index products, MOD13A1 (A Huete et al., 2002) were acquired for each selected site from the Oak Ridge National Laboratory's Distributed Active Archive Center (DAAC) website (http://www.modis.ornl.gov/modis/index.cfm). MOD13A1 data are provided every 16 days at 500 meters spatial resolution as a grid level-3 product in the sinusoidal projection, with radiometric and geometric correction, along with bidirectional effect adjustment and other calibrations (Alfredo Huete, Justice, & Van Leeuwen, 1999). This product was then used to extract NDVI. Cloud contaminated and high aerosol pixels are rejected by selecting the quality flag, which ensures the good quality of NDVI. NDVI was extracted from 5×5 MODIS pixels (2.5 km×2.5 km) that centered on the flux tower, as for the problem of uncertainty in determination which pixel the footprint falls in. All the NDVI pixel values in this 5*5 range with good quality were averaged to one value, and represented the NDVI for the site point.

2.3. AVHRR NDVI dataset (GIMMS)

The GIMMS (Global Inventory Modeling and Mapping Studies) data set is a NDVI product available for a 25 year period spanning from 1981 to 2006, and open to the public by Global Land Cover Facility, University of Maryland (http://glcf.umd.edu/data/gimms/index.shtml). The dataset is derived from imagery obtained from the Advanced Very High Resolution Radiometer (AVHRR) instrument on board of the NOAA satellite series 7, 9, 11, 14, 16 and 17 (Table 2). This is an NDVI dataset that has been corrected for calibration, viewing geometry, volcanic aerosols, and other effects not related to vegetation change (Tucker et al., 2005). The GIMMS collection is available here in two projections: Albers projection with each continent a separate file, or global files in Geographic coordinates. It has a 8 kilometers spatial resolution with half month time interval, which provides 24 scenes for one year. Same with the MODIS NDVI data set, we only chose the pixel with good quality (with quality flag=0). Only the pixel with the flux tower coordinate was used to extract the NDVI value.

Table 2: Comparison between MODIS and AVHRR NDVI Data Sets

NDVI Product		MOD13A1	GIMMS
Sensor		MODIS	AVHRR
Satellite		TERRA and AQUA	NOAA 7, 9, 11, 14, 16 and 17
Bands used	Visible Red	620-670nm	580-680nm
	Near Infrared	841-876nm	725-1000nm
Time interval		16 days	15 days
Spatial resolution		500 meters	8 kilometers
Data Period		February,2000 to now	August,1981 to 2006

2.3. Preprocessing of Ameriflux Data and NDVI data

Since the data period for Ameriflux forest sites we selected are not uniform (Table 1), so as the MODIS (MOD13A1) and AVHRR (GIMMS) NDVI data set (Table 2), only the ground data with

Table 3: Timetable for MODIS (MOD13A1) and AVHRR (GIMMS) NDVI 163 Data and Sites' Measurement. The Grey Boxes Indicate Years of Data Used in this Study

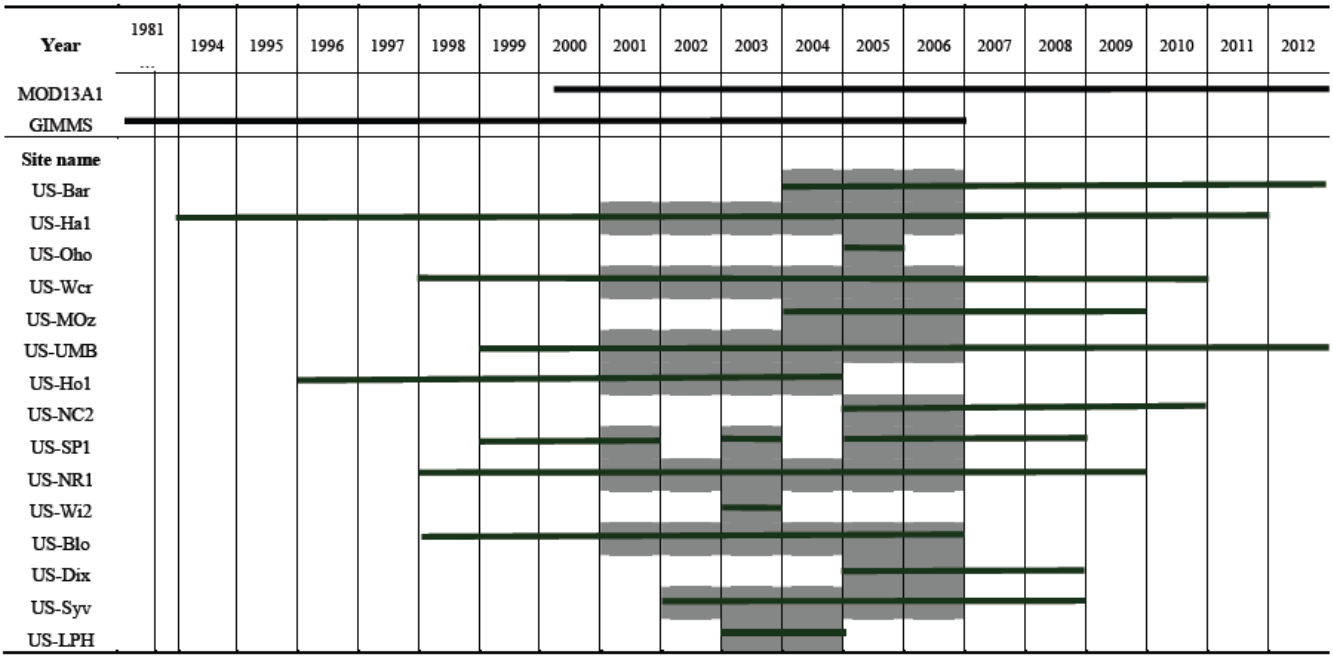

Corresponded remote sensing data were chosen in the study (Table 3). The original data, using the good quality filtering described as above, still have noise and missing point. Thus we applied Savitzky–Golay (SG) filter (Chen et al., 2004; Savitzky & Golay, 1964) to them to get continuous data curves. The SG filter is a moving window least square fitting. In this paper, the window size was 5 and the order of the fitting function was 3. This processing was conducted in Matlab R2013a software (MathWorks Inc.) using TIMESAT package (Jönsson & Eklundh, 2004).

As the MOD13A1 product has 16 days time interval, which gets 23 scenes on year, while the GIMMS product is half month synthesized and 24 scenes for one year (Table 2). For each selected site, we resampled the GIMMS NDVI data into 16 days interval, which means, every 16 calendar day in a year, one NDVI value was generated and 23 values for the whole year. For the Ameriflux data, the daily records of GPP and global radiation (SWR) were summed in 16 days interval (the last data at the end of year is for 13 (common year) or (leap year) days). This processing was also conducted in Matlab R2013a software (MathWorks Inc.). Finally, we obtained 25 years data (575 records) for deciduous broadleaf forest, 23 years data (529 records) for evergreen needleleaf forest and 9 years (207 records) data for mixed forest, which makes 57 years data (1311 records) in total.

The imagery format was uniformed into Geotiff, and the map projection was Albers Conical Equal Area. Low quality data points within the sample window were eliminated. The rest of them were average to the value which can be further analyzed. All these processing accomplished in PCI Geomatica 2012 (PCI Geomatics Inc.).

2.4. Analytical Approach

As indicated in the introduction part, we used the LUE model to analyze the potential of MODIS and AVHRR NDVI data sets for estimating GPP from Ameriflux forests sites. Equation 4, 5 and 6 listed below show those three predictors for the estimation:

$$GPP = f(NDVI) \quad (4)$$

$$GPP = f(NDVI * NDVI) \quad (5)$$

$$GPP = f(NDVI * NDVI * PAR) \quad (6)$$

In addition, three statistical models: linear, quadratic and exponent function were used to establish the relationship between GPP and three predictors (NDVI, NDVI*NDVI and NDVI*NDVI*PAR).

Coefficient of determination (R2) and root mean square error (RMSE) were used to evaluate model's prediction power. First, we established the relationship for deciduous broadleaf forest, evergreen needleleaf forest and mixed forest separately. Then we generated the relationship for all sites in order to determine if there is any difference for various forest types. Akaike Information Criterion (AIC) (Akaike, 1974) and Bayesian Information Criterion (BIC) (Burnham & Anderson, 2004) were used to compare performance of predictor between different statistical models.

$$AIC = 2k + n\ln(SSE/n) \quad (7)$$

$$BIC = 2k * \ln(n) + n\ln(SSE/n) \quad (8)$$

k is the number of parameters used for the statistical model, n is the number of observation, and SSE is the residual sum of squares from that model. AIC deals with the trade-off between the goodness of fit of the model and the complexity of the model. It is founded on information entropy: it offers a relative estimate of the information lost when a given model is used to represent the process that generates the data (Akaike, 1974; Burnham & Anderson, 2004). Both BIC and AIC resolve this problem by introducing a penalty term for the number of parameters in the model. The BIC penalizes the number of parameters more strongly than does the AIC (Liddle, 2007).

Moreover, one-way analysis of variance (ANOVA) was applied to examine the diversity between different models generated from deciduous broadleaf forest, evergreen needleleaf forest, mixed forest and all forest sites, in order to identify if there is one universal model for all types forests. All the analysis were conducted in the RStudio software, version 0.97.312 (RStudio.Inc.).

3. Results and Discussion

The fitting results are shown in Table 4. Linear function, quadratic function and exponent function are illustrated separately, with two different NDVI data sets, three different predictors for deciduous broadleaf forest, evergreen needleleaf forest, mixed forest and all forest sites.

3.1. Comparison between MODIS and AVHRR NDVI Data Sets

Although both MODIS and AVHRR NDVI datasets have the significant power of GPP estimation (Table 4), for all three statistical models and three predictors, the NDVI data from MODIS (MOD13A1) shows better performance than AVHRR data (GIMMS), with higher R^2 and lower RMSE, except for mixed forest with NDVI or NDVI*NDVI as predictor in linear function model, which the GIMMS data has better performance than MODIS data. However, both data sets have significant relation between the selected predictor and GPP. The R2 is 0.73 of MODIS NDVI, while 0.60 for GIMMS NDVI for all types of forests, taking NAVI*NDVI*PAR as predictor. However, the difference between models and predictors are not distinct, which will be discussed in following sections.

Three major aspects are concerned for global or regional satellite remote sensing NDVI data set: spatial/temporal resolution, atmospheric/BRDF (Bidirectional reflectance distribution function) correction effect and obit coherence.

The GIMMS data used here only has 8-kilometers spatial (Table 2) resolution, which introduces mixing pixel (Hsieh, Lee, & Chen, 2001), and it can largely disturb the calculation of NDVI value for the point in central with corresponding flux tower. While MOD13A1 has 500 meters resolution which can provide more detail and represent spatial variation for the same area. As NDVI is a ratio of differences between two adjacent bands (Equation 3), it is largely insensitive to variations in illumination intensity. However, NDVI is sensitive to effects that differ between bands. The GIMMS data set is generated with NOAA7, 9, 11, 14, 16 and 17 from 1981 to 2006. Band calibrations changed frequently between the five NOAA AVHRR instruments that acquired the NDVI record, which caused the spectral response inconsistent problem (Trishchenko, 2009). Even in the mission duration period for one satellite, it would face the issue of spectral degradation (Wang et al., 2012). Those problems related to spectral response reduce the accuracy for GIMMS NDVI dataset.

In addition, natural variability in atmospheric aerosols and column water vapor have affected the NDVI record. Aerosols, along with smoke from biomass burning and dust from soil erosion and other

Table 4: Regression Results for Sites' Based 238 GPP And NDVI. Taking NDVI, NDVI*NDVI, and NDVI*NDVI*PAR as Predictor, Linear Function. ('' Indicate P-Value<0.001, '*' Indicate P Value<0.01). DF: Deciduous Broadleaf Forest, EF: Evergreen Needleleaf Forest, MF: Mixed Forest, all: all Forest Types**

NDVI set		MOD13A1					GIMMS				
Predictor		Function	RMSE	R^2	AIC	BIC	Function	RMSE	R^2	AIC	BIC
X=NDVI	DF	GPP=243.9*X-83.7 **	45.67	0.62	5789	5802	GPP=271.3*X-77.9 **	48.61	0.57	5858	5871
	EF	GPP=172.4*X-54.5 **	40.03	0.35	5408	5421	GPP=181.8*X-51.7 *	43.27	0.24	5491	5503
	MF	GPP=206.5*X-73.2 **	37.42	0.61	2091	2101	GPP=232.9*X-70.3 **	31.69	0.72	2022	2032
	All	GPP=215.4*X-74.9 **	43.09	0.53	13353	13369	GPP=232.1*X-69.4 **	45.66	0.47	13502	13518
X=NDVI*NDVI	DF	GPP=250.4*X-41.4 *	36.47	0.76	5540	5553	GPP=295.2*X-29.0 **	43.90	0.65	5745	5758
	EF	GPP=158.5*X-13.5 **	39.08	0.38	5383	5396	GPP=159.3*X-2.7 **	43.15	0.24	5488	5501
	MF	GPP=207.5*X-34.5 **	30.04	0.75	2000	2010	GPP=234.7*X-23.8 *	26.47	0.81	1947	1957
	All	GPP=215.9*X-33.7 **	38.02	0.63	13030	13046	GPP=238.3*X-21.9 **	43.42	0.52	13372	13388
X=NDVI*NDVI*PAR	DF	GPP=19.5*X-15.2 **	25.59	0.88	5149	5162	GPP=24.1*X-11.9 **	31.48	0.82	5378	5391
	EF	GPP=11.8*X+6.6 **	38.53	0.40	5368	5381	GPP=9.9*X+20.1 *	43.17	0.24	5488	5501
	MF	GPP=17.1*X-13.7 **	19.52	0.90	1821	1831	GPP=18.9*X-6.7 **	20.47	0.88	1841	1851
	All	GPP=16.9*X-10.3 *	32.79	0.73	12649	12664	GPP=18.1*X-1.1 **	40.36	0.59	13184	13200

Table 4: Regression Results for Sites' Based GPP and NDVI, Continued, Quadratic Function

NDVI set		MOD13A1					GIMMS				
Predictor		Function	RMSE	R^2	AIC	BIC	Function	RMSE	R^2	AIC	BIC
X=NDVI	DF	GPP=619.9*X^2-412.1*X+50.8 **	29.67	0.84	5314	5331	GPP=554.2*X^2-262.8*X+25.1 **	42.39	0.67	5708	5725
	EF	GPP=311.3*X^2-175.9*X+32.1 *	38.79	0.39	5376	5393	GPP=148.9*X^2+12.2*X-6.0 *	43.19	0.24	5490	5507
	MF	GPP=546.9*X^2-382.4*X+55.4 **	23.85	0.84	1905	1918	GPP=437.7*X^2-217*X+24.5 **	24.82	0.83	1922	1935
	All	GPP=528*X^2-351.5*X+50.1 *	34.76	0.69	12800	12821	GPP=389.3*X^2-160*X+14.6 *	42.99	0.53	13348	13368
X=NDVI*NDVI	DF	GPP=409.6*X^2-91.5*X+1.4 **	28.63	0.85	5274	5292	GPP=304.2*X^2+89.9*X-8.6 **	42.52	0.67	5711	5728
	EF	GPP=194*X^2+4.2*X+9.7 *	38.39	0.40	5365	5382	GPP=17.51*X^2+146.1*X-0.6 *	43.19	0.24	5490	5507
	MF	GPP=351.3*X^2-86.3*X+4.9 **	22.66	0.86	1884	1897	GPP=179.5*X^2+101.8*X-9.1 **	25.39	0.82	1931	1944
	All	GPP=349.6*X^2-71.5*X+6.1 **	33.55	0.71	12710	12730	GPP=166*X^2+120.6*X-7.8 *	43.01	0.53	13349	13370
X=NDVI*NDVI*PAR	DF	GPP=0.35*X^2+15.9*X-11.9 **	25.4	0.88	5142	5160	GPP=-0.23*X^2+26.6*X-13.9 **	31.48	0.82	5379	5396
	EF	GPP=-1.07*X^2+21.3*X-7.2 *	37.97	0.41	5353	5370	GPP=-1.37*X^2+22.4*X+1.1 *	42.13	0.28	5463	5480
	MF	GPP=0.76*X^2+9.8*X-5.3 **	18.35	0.91	1797	1819	GPP=-0.165*X^2+20.3*X-8.1 **	20.47	0.88	1842	1855
	All	GPP=0.40*X^2+13.0*X-5.4 **	32.61	0.73	12636	12657	GPP=-1.04*X^2+26.7*X-10.9 *	39.68	0.60	13141	13162

Table 4: Regression Results for Sites' Based GPP and NDVI, Continued, Exponent Function

NDVI set		MOD13A1					GIMMS				
Predictor		Function	RMSE	R^2	AIC	BIC	Function	RMSE	R^2	AIC	BIC
X=NDVI	DF	GPP=1.287*exp(5.67*X)-12.65 **	29.47	0.84	5273	5285	GPP=6.878*exp(4.18*X)-21.49 **	42.66	0.67	5692	5730
	EF	GPP=0.7053*exp(5.92*X)+10.83 *	38.11	0.41	5296	5304	GPP=28.1*exp(2.00*X)-39.3 *	43.18	0.24	5780	5803
	MF	GPP=0.7819*exp(6.01*X)-6.274 **	23.2	0.85	1883	1903	GPP=9.078*exp(3.53*X)-24.47 **	25.65	0.81	1911	1934
	All	GPP=0.8673*exp(5.976*X)-3.385 **	33.5	0.72	12735	12770	GPP=9.744*exp(-3.50*X)-22.88 *	43.04	0.51	12809	12986
X=NDVI*NDVI	DF	GPP=21.18*exp(2.96*X)-34.22 **	29.75	0.84	5263	5360	GPP=76.65*exp(1.92*X)-9.27 **	42.64	0.67	5630	5740
	EF	GPP=10.17*exp(3.40*X)+1.19 *	38.02	0.41	5285	5378	GPP=330.9*exp(0.411*X)-329.9 *	43.19	0.24	5987	6013
	MF	GPP=13.85*exp(3.24*X)-20.81 **	23.41	0.85	1876	1913	GPP=110.3*exp(1.29*X)-123.1 **	25.58	0.82	2013	2104
	All	GPP=14.86*exp(3.24*X)-18.84 *	33.55	0.71	12730	13340	GPP=104.4*exp(1.37*X)-113.9 *	43.02	0.53	13287	13320
X=NDVI*NDVI*PAR	DF	GPP=573*exp(0.0291*X)-585.7 **	25.44	0.88	5320	5468	GPP=-1639*exp(-0.016*X)+1625 **	31.49	0.81	5450	5509
	EF	GPP=9502*exp(0.0013*X)-9501 *	38.68	0.39	5560	5678	GPP=10420*exp(0.001*X)-10410 *	43.54	0.23	5977	6018
	MF	GPP=-5449*exp(-0.0032*X)+5435 **	19.66	0.89	1902	2074	GPP=-1315*exp(-0.015*X)+1307 **	20.47	0.88	1989	2039
	All	GPP=0.8673*exp(5.98*X)-3.385 *	33.5	0.72	13767	13675	GPP=7321*exp(0.0024*X)-7322 *	40.41	0.58	12967	13957

factors, can introduce significant variability in the AVHRR NDVI record. These constituents have significantly different effects on AVHRR band 1 and 2. The GIMMS NDVI corrects for the known changes of the atmosphere from two volcanic eruptions (El Chichon in 1982 and Mt. Pinatubo in 1991), but reductions in the NDVI signal can still be seen over densely vegetated tropical land covers for limited time periods (Pinzon, Brown, & Tucker, 2004). However, the MOD13A1 uses MOD09 product for input, which is the atmospheric corrected land surface reflectance.

Three major composite methods: bidirectional reflectance distribution function composite (BRDF-C), constrained-view angle-maximum value composite (CV-MVC) and maximum value composite (MVC) are applied to generate MOD13A1 (A Huete et al., 2002; Alfredo Huete et al., 1999). It ensures the high accuracy for MODIS NDVI dataset.

Furthermore, the AVHRR sensor has the orbit drifting problem caused by the change in solar zenith angle (SZA). And it affects the determination of solar-observation geometry, which leads to the difficulty for BRDF correction of land surface target (Kaufmann et al., 2000). While the MODIS sensor does not have that problem and has a coherent orbit. All these reasons make the MODIS NDVI data set outperform AVHRR data set. However, it has the global record only from 1999. Therefore, several studies has tried to compare different NDVI dataset , and they provided the chance of calibration different NDVI data sets for global biology monitoring for long time period.

3.2. Assessment for Different Predictors

We took three predictors, including NDVI, NDVI*NDVI and NDVI*NDVI*PAR for estimation of GPP. Though all of them can be used to generate significant regression functions with GPP for selected statistical models, the general trend for these three predictors shows that NDVI*NDVI*PAR has the best performance with higher R^2 and lower RMSE (Table 4). Which gets the NDVI*NDVI has the second best power for GPP estimation while the NDVI has the relatively weaker power.

As mentioned in the introduction part, the NDVI is a proxy for vegetation canopy physical and physiological parameters, such as fAPAR , LAI, chlorophyll content and so on. Moreover, PAR is with great spatial and temporal variation. Thus, Sims *et al.* explored using the temperature and greenness (TG) model to estimate GPP, based on the enhanced vegetation index (EVI) and the land surface temperature (LST) (Sims et al., 2008). LST is considered to have inner correlation with both vapor pressure deficit (VPD) and PAR. Combination of EVI and LST in the model substantially improved the correlation between the predicted and measured GPP at flux towers in a wide range of vegetation types across North America and provided substantially better predictions of GPP than the MODIS GPP product (Sims et al., 2006). Wu *et al.* proposed a new vegetation index (VI) model for GPP estimation, which incorporated vegetation indices for both LUE and fAPAR estimation land at first, and expanded to forest later, which got reasonable results.

These previous studies suggested that vegetation indices can be used as proxies for GPP estimation while PAR also plays an important role in the LUE model (Equation 1), which controls the component for incoming solar radiation. Therefore, it explains the reason why the NDVI*NDVI*PAR is the best predictor in our research. However, there is a lack of remote sensing based global PAR product, especially for fine resolution and high temporal resolution of long time period (Pinker & Laszlo, 1992 X. Zhao et al., 2013), which limited the expansion for LUE model globally. Based on our study, GPP can be estimated by correlating in situ GPP with NDVI and this method worked well in some other studies. Gitelson maize from Landsat data with R (WDRVI) (Anatoly A Gitelson et al., 2008. Wu et al. tested this approach by comparing NDVI, EVI, WDRVI and SAVI (soil adjust vegetation index) for MODIS data and found out that the EVI had best correlation with GPP (C. Wu, Niu, et al., 2010 to explore the relationship between GPP and VI in the paper, since GIMMS only provides NDVI data. However, the result is still reasonable by statistical models, which indicates only taking NDVI from MODIS and GIMMS datasets can be applied to GPP estimation. With 25 years duration of GIMMS dataset, and hopefully extended to the future, it is beneficial for long time period GPP estimation.

Figure 2: Regression lines of GPP vs. NDVI*NDVI*PAR for DF, EF, MF and All forest for MODIS (MOD13A1) and AVHRR (GIMMS) Data Sets

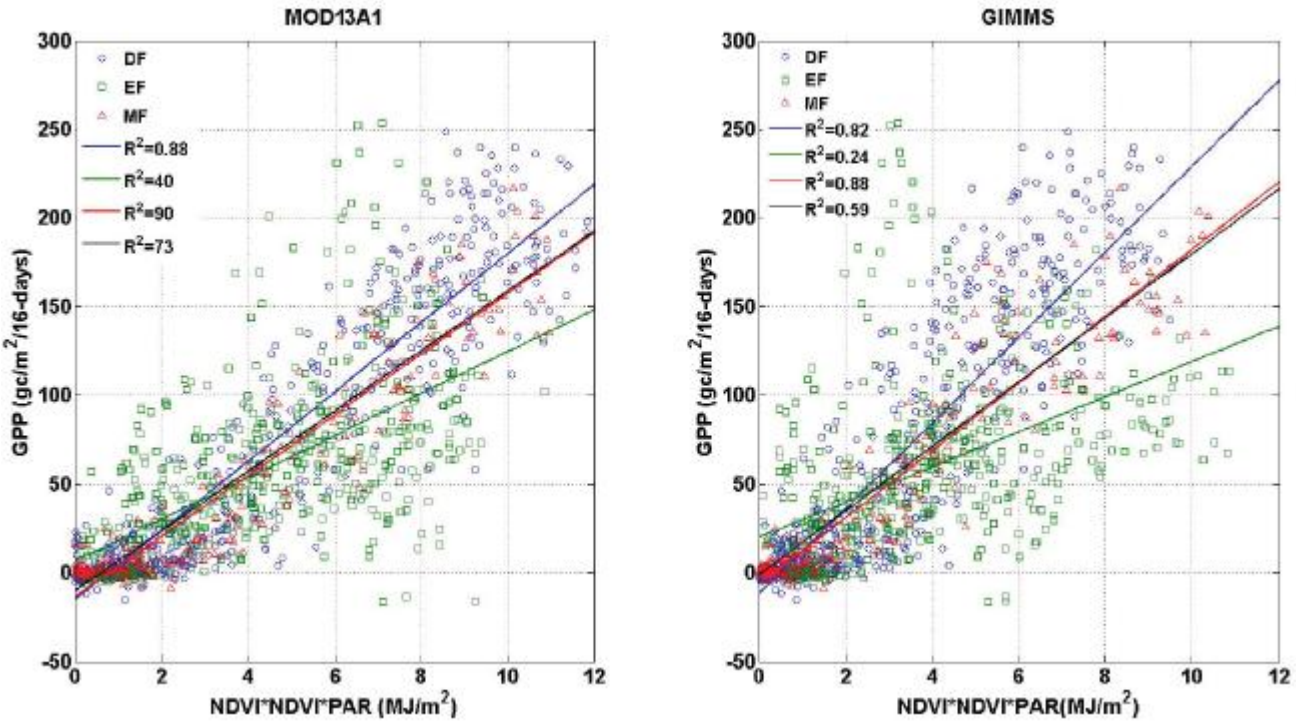

3.3. Comparison between three Statistical Models

Linear, quadratic and exponent function were used to establish the relationship between GPP and NDVI in this study. Table 4 shows that for both MODIS and GIMMS data sets, the exponent function has the lowest AIC (12735 for MODIS and 12809 for GIMMS) and BIC (12770 for MODIS and 12986 for GIMMS), taking NDVI as predictor, which suggests that it has better performance in this situation. The quadratic function has lower AIC (12636 for MODIS and 13141 for GIMMS) and BIC (12657 for MODIS and 13162 for GIMMS) than exponent function for two data sets, taking NDVI*NDVI*PAR as predictor. However, differences between quadratic and linear function in AIC and BIC are not so obvious, so as the R^2 and RMSE. It indicates that both linear function and quadratic function have the power to generate the relationship between GPP and NDVI*NDVI*PAR. For NDVI*NDVI, the quadratic function has lower AIC (12710) and BIC (12730) for MODIS data set, while the exponent has lower AIC (13287) and BIC (13320) for GIMMS data set. But differences in R^2 and RMSE is still not distinct.

Nonlinear relationship is found out between single vegetation index and GPP for many vegetation types, and the exponent function is widely used to describe this relationship, which explains why it is better than other functions in this study, taking only NDVI as predictor. In previous study, it is also proved that the VI*VI*PAR has linear relationship with in situ GPP (Anatoly A Gitelson et al., 2008; Anatoly A. Gitelson et al., 2006; C. Wu, Niu, et al., 2010). Wu *et al.* suggested that this combination can introduce more errors for GPP estimation, since the noise behind vegetation index has been amplified, especially for the vegetation index data set with obvious background noise (C. Wu, Munger, Niu, & Kuang, 2010; C. Wu, Niu, et al., 2010). In this study, the evergreen forest sites have more discretization (Figure 2), which gets lower R^2 and higher RMSE. Meanwhile, as PAR is an important component for GPP estimation, and the form of NDVI*NDVI takes LUE and fAPAR into the consideration. This combination leads to the predictor: NDVI*NDVI*PAR, which decreases the fitting power of exponent function suitable for single VI, and increases the fitting power for linear function slightly. However, the linear function is thought to have universal explanatory power because it only needs two parameters. The results for the linear fitting between GPP and NDVI*NDVI*PAR for two data sets are shown in Figure 2.

3.4. Comparison between Different Forest Types

Both deciduous broadleaf forest (DF) and mixed forest (MF) have better regression accuracy than evergreen needleleaf forest (EF) for all predictors and all three statistical models (Table 4).

Figure 2 also shows that the discreteness between NDVI*NDVI*PAR and GPP for EF is obviously larger than DF and MF.

Figure 3: Annual NDVI Variation and Standard Deviation for Nearby Pixels of Cary Site (US-SP1)

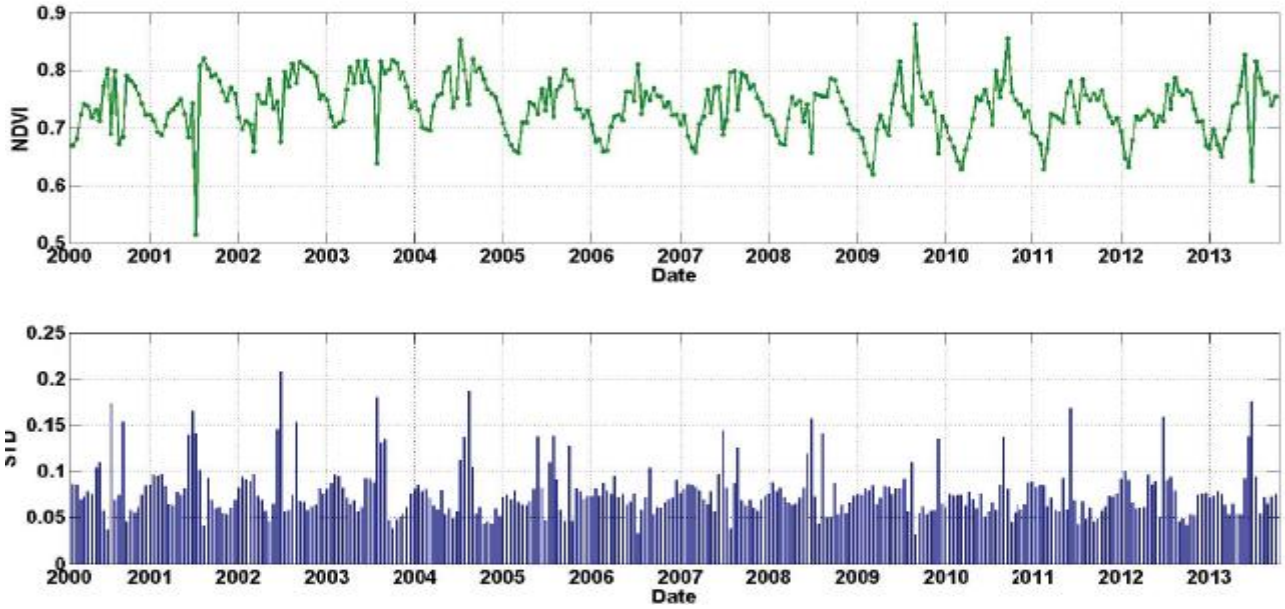

We checked the original NDVI series for six selected evergreen needleleaf forest sites and figured out that the Austin Cary site (US-SP1) has the abnormal discreteness situation (Figure 3).

The location for this site is at 29.7381N, 82.2188W, Florida, which falls into the subtropical zones, with dry mild winters (November- March), warm dry springs (April and May), warm humid summers (June-October), with 52% of total precipitation falling during the summer months (Gholz et al., 1991). The annual average NDVI is larger than 0.65, except for several outliers. It makes small seasonal change for this site.

From the standard derivation derived for the nearby area where we made a subset, it shows that the NDVI has obvious fluctuation and it disturbs the regression between GPP and NDVI data. This result is consistent with previous studies. Hashimoto *et al.* explored simple algorithms for estimating GPP in forest areas from satellite data and figured out that the evergreen forest has poorer regression accuracy than deciduous forest, while tropical forest has the poorer regression accuracy compared with non-tropical forest reason (Hashimoto et al., 2012). The reason is that there is small seasonal changes observed in evergreen and tropical forest leaves, which are smaller than the inter annual variation in leaf phenology (AR Huete et al., 2008). Furthermore, the problem of saturation of NDVI has been disclosed by other researches (Gutman & Ignatov, 1998; A. R. Huete, Liu, & van Leeuwen, 1997). It shows that the NDVI is not sensitive to spectral signal due to high density vegetation cover after a certain threshold. That also limits the application for GPP estimation by NDVI in high density vegetation covered area.

.

Table 5: ANOVA Test Results for Models between all Types Forest and DF, EF, MF, with Corresponding Predictor of Linear, Quadratic and Exponent Function for MODIS (MOD13A1) and AVHRR (GIMMS) Data Sets

Linear		MOD13A1		GIMMS	
Predictor		F-value	P-value	F-value	P-value
NDVI	DF v ALL	6.38	0.0117	14.35	0.0002
	EF v ALL	12.01	0.0005	49.29	0
	MF v ALL	0.59	0.4446	0.01	0.9225
NDVI*NDVI	DF v ALL	3.33	0.0481	10.46	0.0013
	EF v ALL	4.67	0.0309	25.9	0
	MF v ALL	0.66	0.4186	0.55	0.4606
NDVI*NDVI *PAR	DF v ALL	1.92	0.1667	4.03	0.045
	EF v ALL	3.3	0.0697	14.28	0.0002
	MF v ALL	0.23	0.6335	0.35	0.5564

Quadratic		MOD13A1		GIMMS	
Predictor		F-value	P-value	F-value	P-value
NDVI	DF v ALL	50.93	0	176.57	0
	EF v ALL	726.95	0	1405.34	0
	MF v ALL	0.24	0.6263	1.27	0.2604
NDVI*NDVI	DF v ALL	6.7	0.0097	61.29	0
	EF v ALL	119.61	0	296.63	0
	MF v ALL	0.96	0.3291	0.21	0.6437
NDVI*NDVI *PAR	DF v ALL	2.25	0.1343	0.05	0.8226
	EF v ALL	90.82	0	1.74	0.1876
	MF v ALL	7.1	0.008	4.15	0.0423

Exponent		MOD13A1		GIMMS	
Predictor		F-value	P-value	F-value	P-value
NDVI	DF v ALL	0.12	0.7327	1051.15	0
	EF v ALL	0.69	0.4062	5268.8	0
	MF v ALL	1.6	0.2061	351.8	0
NDVI*NDVI	DF v ALL	0.04	0.8387	784.04	0
	EF v ALL	0.48	0.4887	12.41	0.0004
	MF v ALL	1.6	0.2072	0.88	0.3496
NDVI*NDVI *PAR	DF v ALL	3.71	0.0542	6.72	0.0097
	EF v ALL	1.96	0.1618	46.32	0
	MF v ALL	4.23	0.0404	0.42	0.5156

Another issue related to GPP estimation for different forest types is the variance in model specification. The MODIS GPP product which based on the Biome-BGC model (Running et al., 2000; Turner et al., 2006) uses lookup table to deal with this issue. The deciduous forest and evergreen forest use two sets of parameters in this model, which indicates those two types of forest have different photosynthesis feature and carbon fixation ability. We used one-way analysis of variance (ANOVA) to test the significant of difference between different models (linear, quadratic and exponential) generated from DF, EF, MF and all forest types. The results are shown in Table 5. With 95% confidence, except for exponent model taking NDVI and NDVI*NDVI as predictors from MODIS dataset, there are significant differences in GPP estimation models for these three forest types.

However, the difference between MF and all forest types is not significant, which suggests that different forest types require different sets of parameters for GPP estimation and the MF has better coherence with all forest types. Taking NDVI*NDVI*PAR as predictor, there is no significant difference between different forest types in three models for MODIS dataset, except for evergreen forest and mixed forest of quadratic model (p=0 and p=0.008), and mixed forest of exponential model (p=0.0404). As for GIMMS dataset, significant difference is between different forest types and all forest data, except for mixed forest from linear and exponential model, deciduous forest and evergreen forest from quadratic model. That indicated the NDVI*NDVI*PAR has better performance of uniforming parameters for GPP estimation in different forest types. Wu *et al.* also figured out the difference of GPP estimation for deciduous forest sites and evergreen forest sites and developed a parameterization method, using dEVI and LST for different vegetation types (C. Wu et al., 2014; C. Y. Wu & Niu, 2012). In this study, we explored the potential for using one set of parameters to estimate GPP for different forest types. The NDVI*NDVI*PAR has the potential to uniform parameters for GPP estimations, while exceptions happens as model selection varies, suggesting that it needs cautious consideration for both model and predictor selection.

4. Conclusions

We investigated the potential of MODIS and AVHRR NDVI datasets for gross primary productivity estimation for three different forest types, over the continental U.S. The results show that both MODIS data set (MOD13A1) and AVHRR data set (GIMMS) have the ability to estimate GPP for selected forests sites. Due to data quality and spatial resolution issues, the MOD13A1 data has better overall performance than the GIMMS data. Furthermore, the estimation accuracy varies with different predictors. Taking photosynthetically active radiation (PAR) into account, the predictor of NDVI*NDVI*PAR has the best power for GPP estimation. The predictor of NDVI and NDVI*NDVI also have reasonable estimation ability for GPP. However, the three factor multiple form may introduce uncertainty because of noise in NDVI data set. Very few improvement has been detected for quadratic function and exponent function, compared with linear function. It indicates that the linear function is qualified for generating the relationship between GPP and NDVI data, especially for the predictor of NDVI*NDVI*PAR. Obvious difference is found between broadleaf forest, evergreen needleleaf forest and mixed forest sites, indicating that the carbon fixation feature for different types forest varies, while the predictor of NDVI*NDVI*PAR has the potential for uniforming parameters of GPP estimation. However, it needs cautious consideration for the regression model selection.

Acknowledgments

We sincerely appreciate the help of the researchers affiliated with the FLUXNET network.

We are grateful to The Global Land Cover Facility (GLCF) for providing the GIMMS data and the Oak Ridge National Laboratory Distributed Active Archive Center (ORNL DAAC) for MODIS (MOD13A1) data. This study was funded by Chinese Scholarship Council (CSC).

Conflicts of Interest The authors declare no conflict of interest.

References

Abella, S. R., Jaeger, J. F., Gehring, D. H., Jacksy, R. G., Menard, K. S., & High, K. A. (2001). Restoring historic plant communities in the Oak Openings region of northwest Ohio. *Ecological Restoration, 19*(3), 155-160.

Akaike, H. (1974). A new look at the statistical model identification. *Automatic Control, IEEE Transactions on, 19*(6), 716-723.

Bolstad, P., Davis, K., Martin, J., Cook, B., & Wang, W. (2004). Component and whole-system respiration fluxes in northern deciduous forests. *Tree Physiology, 24*(5), 493-504.

Brosofske, K., Chen, J., & Crow, T. R. (2001). Understory vegetation and site factors: implications for a managed Wisconsin landscape. *Forest Ecology And Management, 146*(1), 75-87.

Burnham, K. P., & Anderson, D. R. (2004). Multimodel inference understanding AIC and BIC in model selection. *Sociological methods & research, 33*(2), 261-304.

Chen, J., Jönsson, P., Tamura, M., Gu, Z., Matsushita, B., & Eklundh, L. (2004). A simple method for reconstructing a high-quality NDVI time-series data set based on the Savitzky–Golay filter. *Remote Sensing Of Environment, 91*(3–4), 332-344. doi: http://dx.doi.org/10.1016/j.rse.2004.03.014

Clark, K. L., Skowronski, N., Hom, J., Duveneck, M., Pan, Y., Van Tuyl, S., . . . Maurer, S. (2009). Decision support tools to improve the effectiveness of hazardous fuel reduction treatments in the New Jersey Pine Barrens. *International Journal Of Wildland Fire, 18*(3), 268-277.

Coops, N. C., Waring, R. H., & Law, B. E. (2005). Assessing the past and future distribution and productivity of ponderosa pine in the Pacific Northwest using a process model, 3-PG. *Ecological Modelling, 183*(1), 107-124. doi: http://dx.doi.org/10.1016/j.ecolmodel.2004.08.002

Curtis, P. S., Hanson, P. J., Bolstad, P., Barford, C., Randolph, J., Schmid, H., & Wilson, K. B. (2002). Biometric and eddy-covariance based estimates of annual carbon storage in five eastern North American deciduous forests. *Agricultural And Forest Meteorology, 113*(1), 3-19.

DeForest, J., Sun, G., Noormets, A., Chen, J., McNulty, S., Gavazzi, M., . . . Skaggs, R. (2006). *Carbon and water fluxes in a drained coastal clearcut and a pine plantation in eastern North Carolina.* Paper presented at the Proceedings of the International Conference.

Desai, A. R., Bolstad, P. V., Cook, B. D., Davis, K. J., & Carey, E. V. (2005). Comparing net ecosystem exchange of carbon dioxide between an old-growth and mature forest in the upper Midwest, USA. *Agricultural And Forest Meteorology, 128*(1), 33-55.

Fensholt, R., & Proud, S. R. (2012). Evaluation of Earth Observation based global long term vegetation trends — Comparing GIMMS and MODIS global NDVI time series. *Remote Sensing Of Environment, 119*(0), 131-147. doi: http://dx.doi.org/10.1016/j.rse.2011.12.015

Gallo, K., Ji, L., Reed, B., Dwyer, J., & Eidenshink, J. (2004). Comparison of MODIS and AVHRR 16-day normalized difference vegetation index composite data. *Geophysical Research Letters, 31*(7).

Gholz, H., Vogel, S., Cropper Jr, W., McKelvey, K., Ewel, K., Teskey, R., & Curran, P. (1991). Dynamics of canopy structure and light interception in Pinus elliottii stands, north Florida. *Ecological Monographs*, 33-51.

Gitelson, A. A., Viña, A., Masek, J. G., Verma, S. B., & Suyker, A. E. (2008). Synoptic monitoring of gross primary productivity of maize using Landsat data. *Geoscience and Remote Sensing Letters, IEEE, 5*(2), 133-137.

Gitelson, A. A., Viña, A., Verma, S. B., Rundquist, D. C., Arkebauer, T. J., Keydan, G., . . . Suyker, A. E. (2006). Relationship between gross primary production and chlorophyll content in crops: Implications for the synoptic monitoring of vegetation productivity. *Journal Of Geophysical Research, 111*(D8), D08S11. doi: 10.1029/2005jd006017

Goldstein, A. H., & Schade, G. W. (2000). Quantifying biogenic and anthropogenic contributions to acetone mixing ratios in a rural environment. *Atmospheric Environment, 34*(29), 4997-5006.

Gutman, G., & Ignatov, A. (1998). The derivation of the green vegetation fraction from NOAA/AVHRR data for use in numerical weather prediction models. *International Journal Of Remote Sensing, 19*(8), 1533-1543.

Hadley, J. L., Kuzeja, P. S., Daley, M. J., Phillips, N. G., Mulcahy, T., & Singh, S. (2008). Water use and carbon exchange of red oak-and eastern hemlock-dominated forests in the northeastern USA: implications for ecosystem-level effects of hemlock woolly adelgid. *Tree Physiology, 28*(4), 615-627.

Hashimoto, H., Wang, W., Milesi, C., White, M. A., Ganguly, S., Gamo, M., . . . Nemani, R. R. (2012). Exploring Simple Algorithms for Estimating Gross Primary Production in Forested Areas from Satellite Data. *Remote Sensing, 4*(1), 303-326.

Holben, B. N. (1986). Characteristics of maximum-value composite images from temporal AVHRR data. *International Journal Of Remote Sensing, 7*(11), 1417-1434. doi: 10.1080/01431168608948945

Hollinger, D., Goltz, S., Davidson, E., Lee, J., Tu, K., & Valentine, H. (1999). Seasonal patterns and environmental control of carbon dioxide and water vapour exchange in an ecotonal boreal forest. *Global Change Biology, 5*(8), 891-902.

Hsieh, P.-F., Lee, L. C., & Chen, N.-Y. (2001). Effect of spatial resolution on classification errors of pure and mixed pixels in remote sensing. *Geoscience and Remote Sensing, IEEE Transactions on, 39*(12), 2657-2663.

Huete, A., Didan, K., Miura, T., Rodriguez, E. P., Gao, X., & Ferreira, L. G. (2002). Overview of the radiometric and biophysical performance of the MODIS vegetation indices. *Remote Sensing Of Environment, 83*(1), 195-213.

Huete, A., Justice, C., & Van Leeuwen, W. (1999). MODIS vegetation index (MOD13). *Algorithm theoretical basis document*.

Huete, A., Restrepo-Coupe, N., Ratana, P., Didan, K., Saleska, S., Ichii, K., . . . Gamo, M. (2008). Multiple site tower flux and remote sensing comparisons of tropical forest dynamics in Monsoon Asia. *Agricultural And Forest Meteorology, 148*(5), 748-760.

Huete, A. R., Liu, H., & van Leeuwen, W. J. (1997). *The use of vegetation indices in forested regions: issues of linearity and saturation.* Paper presented at the Geoscience and Remote Sensing, 1997. IGARSS'97. Remote Sensing-A Scientific Vision for Sustainable Development., 1997 IEEE International.

Jiang, Z., Huete, A. R., Didan, K., & Miura, T. (2008). Development of a two-band enhance dvegetation index without a blue band. *Remote Sensing Of Environment, 112*(10), 3833- 3845. doi: 10.1016/j.rse.2008.06.006

Jönsson, P., & Eklundh, L. (2004). TIMESAT—A program for analyzing time-series of satellite sensor data. *Computers & Geosciences, 30*(8), 833-845.

Julien, Y., & Sobrino, J. A. (2009). Global land surface phenology trends from GIMMS database. *International Journal Of Remote Sensing, 30*(13), 3495-3513. doi: 10.1080/01431160802562255

Kaufmann, R. K., Zhou, L., Knyazikhin, Y., Shabanov, V., Myneni, R. B., & Tucker, C. J. (2000). Effect of orbital drift and sensor changes on the time series of AVHRR vegetation index data. *Geoscience and Remote Sensing, IEEE Transactions on, 38*(6), 2584-2597.

Liddle, A. R. (2007). Information criteria for astrophysical model selection. *Monthly Notices of the Royal Astronomical Society: Letters, 377*(1), L74-L78.

MÄKELÄ, A., Pulkkinen, M., Kolari, P., Lagergren, F., Berbigier, P., Lindroth, A., . . . Hari, P.(2008). Developing an empirical model of stand GPP with the LUE approach: analysis of eddy covariance data at five contrasting conifer sites in Europe. *Global Change Biology, 14*(1), 92-108.

Monteith, J. (1972). Solar radiation and productivity in tropical ecosystems. *Journal Of Applied Ecology, 9*(3), 747-766.

Monteith, J., & Moss, C. (1977). Climate and the efficiency of crop production in Britain [and discussion]. *Philosophical Transactions of the Royal Society of London. B, Biological Sciences, 281*(980), 277-294.

Myneni, R. B., Hall, F. G., Sellers, P. J., & Marshak, A. L. (1995). The interpretation of spectral vegetation indexes. *Geoscience and Remote Sensing, IEEE Transactions on, 33*(2), 481-486.

Nemani, R. R., Keeling, C. D., Hashimoto, H., Jolly, W. M., Piper, S. C., Tucker, C. J., . . .Running, S. W. (2003). Climate-driven increases in global terrestrial net primary production from 1982 to 1999. *Science, 300*(5625), 1560-1563.

Papale, D., & Valentini, R. (2003). A new assessment of European forests carbon exchanges by eddy fluxes and artificial neural network spatialization. *Global Change Biology, 9*(4), 525-535.

Pinker, R., & Laszlo, I. (1992). Global distribution of photosynthetically active radiation as observed from satellites. *Journal Of Climate, 5*, 56-65.

Pinzon, J., Brown, M., & Tucker, C. (2004). Global Inventory Modeling and Mapping Studies (GIMMS) AVHRR 8-km Normalized Difference Vegetation Index (NDVI) dataset.

Product Guide. Potter, C., Klooster, S., Myneni, R., Genovese, V., Tan, P.-N., & Kumar, V. (2003). Continentalscale comparisons of terrestrial carbon sinks estimated from satellite data and ecosystem modeling 1982–1998. *Global And Planetary Change, 39*(3), 201-213.

Prince, S. D., & Goward, S. N. (1995). Global primary production: a remote sensing approach. *Journal Of Biogeography*, 815-835.

Reichstein, M., Falge, E., Baldocchi, D., Papale, D., Aubinet, M., Berbigier, P., . . . Granier, A. (2005). On the separation of net ecosystem exchange into assimilation and ecosystem respiration: review and improved algorithm. *Global Change Biology, 11*(9), 1424-1439.

Richardson, A. D., Jenkins, J. P., Braswell, B. H., Hollinger, D. Y., Ollinger, S. V., & Smith, M.- L. (2007). Use of digital webcam images to track spring green-up in a deciduous broadleaf forest. *Oecologia, 152*(2), 323-334.

Ruimy, A., Kergoat, L., & Bondeau, A. (1999). Comparing global models of terrestrial net primary productivity (NPP): Analysis of differences in light absorption and light-use efficiency. *Global Change Biology, 5*(S1), 56-64.

Running, S. W., & Gower, S. T. (1991). FOREST-BGC, a general model of forest ecosystem processes for regional applications. II. Dynamic carbon allocation and nitrogen budgets. *Tree Physiology, 9*(1-2), 147-160.

Running, S. W., Nemani, R., Glassy, J. M., & Thornton, P. E. (1999). MODIS daily photosynthesis (PSN) and annual net primary production (NPP) product (MOD17) Algorithm Theoretical Basis Document. *University of Montana, SCF At-Launch Algorithm ATBD Documents (available online at: www. ntsg. umt. edu/modis/ATBD/ATBD_MOD17_v21. pdf)*.

Running, S. W., Thornton, P. E., Nemani, R., & Glassy, J. M. (2000). Global terrestrial gross and net primary productivity from the Earth Observing System. *Methods in ecosystem science*, 44-57.

Salomonson, V. V., Barnes, W., Xiong, J., Kempler, S., & Masuoka, E. (2002). *An overview of the Earth Observing System MODIS instrument and associated data systems performance.* Paper presented at the Geoscience and Remote Sensing Symposium, 2002. IGARSS'02. 2002 IEEE International.

Savitzky, A., & Golay, M. J. (1964). Smoothing and differentiation of data by simplified least squares procedures. *Analytical Chemistry, 36*(8), 1627-1639.

Sims, D. A., Rahman, A. F., Cordova, V. D., El-Masri, B. Z., Baldocchi, D. D., Bolstad, P. V., . .. Xu, L. (2008). A new model of gross primary productivity for North American ecosystems based solely on the enhanced vegetation index and land surface temperature from MODIS. *Remote Sensing Of Environment, 112*(4), 1633-1646. doi: 10.1016/j.rse.2007.08.004

Sims, D. A., Rahman, A. F., Cordova, V. D., El-Masri, B. Z., Baldocchi, D. D., Flanagan, L. B., .. . Xu, L. (2006). On the use of MODIS EVI to assess gross primary productivity of North American ecosystems. *Journal Of Geophysical Research, 111*(G4), G04015. doi: 10.1029/2006jg000162

Trishchenko, A. P. (2009). Effects of spectral response function on surface reflectance and NDVI measured with moderate resolution satellite sensors: Extension to AVHRR NOAA-17, 18 and METOP-A. *Remote Sensing Of Environment, 113*(2), 335-341. doi: http://dx.doi.org/10.1016/j.rse.2008.10.002

Tucker, C. J., Pinzon, J. E., Brown, M. E., Slayback, D. A., Pak, E. W., Mahoney, R., . . . El Saleous, N. (2005). An extended AVHRR 8-km NDVI dataset compatible with MODIS and SPOT vegetation NDVI data. *International Journal Of Remote Sensing, 26*(20), 4485-4498. doi: 10.1080/01431160500168686

Turner, D. P., Ritts, W. D., Cohen, W. B., Gower, S. T., Running, S. W., Zhao, M., . . . Saleska, S. R. (2006). Evaluation of MODIS NPP and GPP products across multiple biomes. *Remote Sensing Of Environment, 102*(3), 282-292.

Turnipseed, A., Blanken, P., Anderson, D., & Monson, R. (2002). Energy budget above a highelevation subalpine forest in complex topography. *Agricultural And Forest Meteorology, 110*(3), 177-201.

Wang, D., Morton, D., Masek, J., Wu, A., Nagol, J., Xiong, X., . . . Wolfe, R. (2012). Impact of sensor degradation on the MODIS NDVI time series. *Remote Sensing Of Environment, 119*(0), 55-61. doi: 10.1016/j.rse.2011.12.001

Wofsy, S., Goulden, M., Munger, J., Fan, S., Bakwin, P., Daube, B., . . . Bazzaz, F. (1993). Net exchange of CO 2 in a mid-latitude forest. *Science, 260*(5112), 1314-1317.

Wu, C., Chen, J. M., & Huang, N. (2011). Predicting gross primary production from the enhanced vegetation index and photosynthetically active radiation: Evaluation and calibration. *Remote Sensing Of Environment, 115*(12), 3424-3435. doi: 10.1016/j.rse.2011.08.006

Wu, C., Gonsamo, A., Zhang, F., & Chen, J. M. (2014). The potential of the greenness and radiation (GR) model to interpret 8-day gross primary production of vegetation. *Isprs Journal Of Photogrammetry And Remote Sensing, 88*(0), 69-79. doi: http://dx.doi.org/10.1016/j.isprsjprs.2013.10.015

Wu, C., Munger, J. W., Niu, Z., & Kuang, D. (2010). Comparison of multiple models for estimating gross primary production using MODIS and eddy covariance data in Harvard Forest. *Remote Sensing Of Environment, 114*(12), 2925-2939. doi: DOI: 10.1016/j.rse.2010.07.012

Wu, C., Niu, Z., & Gao, S. (2010). Gross primary production estimation from MODIS data with vegetation index and photosynthetically active radiation in maize. *Journal Of Geophysical Research, 115*(D12), D12127. doi: 10.1029/2009jd013023

Wu, C., Niu, Z., Tang, Q., Huang, W., Rivard, B., & Feng, J. (2009). Remote estimation of gross primary production in wheat using chlorophyll-related vegetation indices. *Agricultural And Forest Meteorology, 149*(6–7), 1015-1021. doi: 10.1016/j.agrformet.2008.12.007

Wu, C. Y., & Niu, Z. (2012). Modelling light use efficiency using vegetation index and land surface temperature from MODIS in Harvard Forest. *International Journal Of Remote Sensing, 33*(7), 2261-2276. doi: 10.1080/01431161.2011.608090

Xiao, J., Zhuang, Q., Baldocchi, D. D., Law, B. E., Richardson, A. D., Chen, J., . . . Ma, S. (2008). Estimation of net ecosystem carbon exchange for the conterminous United States by combining MODIS and AmeriFlux data. *Agricultural And Forest Meteorology, 148*(11), 1827-1847.

Xiao, X., Zhang, Q., Braswell, B., Urbanski, S., Boles, S., Wofsy, S., . . . Ojima, D. (2004). Modeling gross primary production of temperate deciduous broadleaf forest using satellite images and climate data. *Remote Sensing Of Environment, 91*(2), 256-270.

Yang, B., Hanson, P. J., Riggs, J. S., Pallardy, S. G., Heuer, M., Hosman, K. P., . . . Gu, L.-H. (2007). Biases of CO2 storage in eddy flux measurements in a forest pertinent to vertical configurations of a profile system and CO2 density averaging. *Journal Of Geophysical Research, 112*(D20), D20123.

Yuan, W., Liu, S., Yu, G., Bonnefond, J.-M., Chen, J., Davis, K., . . . Verma, S. B. (2010). Global estimates of evapotranspiration and gross primary production based on MODIS and global meteorology data. *Remote Sensing Of Environment, 114*(7), 1416-1431. doi: 10.1016/j.rse.2010.01.022

Yuan, W. P., Liu, S., Zhou, G. S., Zhou, G. Y., Tieszen, L. L., Baldocchi, D., . . . AmeriFlux, C. (2007). Deriving a light use efficiency model from eddy covariance flux data for predicting daily gross primary production across biomes. *Agricultural And Forest Meteorology, 143*(3-4), 189-207. doi: 10.1016/j.agrformet.2006.12.001

Zhao, M., Running, S. W., & Nemani, R. R. (2006). Sensitivity of Moderate Resolution Imaging Spectroradiometer (MODIS) terrestrial primary production to the accuracy of meteorological reanalyses. *Journal of Geophysical Research: Biogeosciences (2005– 2012), 111*(G1).

Zhao, X., Liang, S., Liu, S., Yuan, W., Xiao, Z., Liu, Q., . . . Zhang, X. (2013). The Global Land Surface Satellite (GLASS) Remote Sensing Data Processing System and Products. *Remote Sensing, 5*(5), 2436-2450.